한국추진공학회 2004년도 추계학술대회 논문집 pp.47~52 2004 KSPE Fall Conference

HyShot 스크램제트 엔진의 흡입구 유동특성 연구

원수희* · 최정열** · 정인석*

Intake Flow Characteristics of HyShot Scramjet Engine

Su-Hee Won* · Jeong-Yeol Choi** · In-Seuck Jeung*

ABSTRACT

In the design of scramjet intake for hypersonic flight, a variety of aerothermodynamics phenomena are encountered. These phenomena include blunt leading - edge effects, boundary layer development issues, transition, inviscid / viscous coupling, shock - shock interactions, shock / boundary - layer interactions, and flow profile effects. For intakes that are designed to operate within a narrow Mach number / altitude envelope, an understanding of a few of these phenomena might be required. In this work several predominant flowfield phenomena (viscous phenomena, boundary - layer separation, and combustor entrance profile) are discussed to investigate the performance of the intake at the altitude and angle of attack extremes of the HyShot flight experiment.

초 록

극초음속 스크램제트 흡입구의 설계는 다양한 공기열역학적인 현상을 수반한다. 이러한 현상은 무딘 앞전효과, 경계층 발달 문제, 천이, 점성/비점성 결합, 충격파 상호작용, 충격파 경계층 상호작용 및 유동 형상 등을 포함한다. 한정된 마하수와 고도 영역 내에서 운용되기 위해 설계되는 흡입구에서는 이러한 현상들 중 몇 가지 현상에 대한 이해가 요구된다. 본 연구에서는 HyShot 비행시험에서 발생할 수 있는 고도와 받음각 극단에서의 흡입구 성능을 연구하기 위해 몇 가지 중요한 유동 현상(점성 현상, 경계층 박리, 연소기 입구 유동 형상)들이 논의 될 것이다.

Key Words: Altitude(고도), AOA(받음각), Boundary-Layer(경계층), Total Pressure Recovery(전압력 회복)

1. Introduction

At the Centre for Hypersonics of The University of Queensland, scramjet research has

* 서울대학교 항공우주공학과
** 부산대학교 항공우주공학과
연락저자, E-mail: enjis@snu.ac.kr

been carried out using ground based experiments in the T4 free piston shock tunnel. The flight test (HyShot) was carried out, in which a small two-dimensional scramjet was mounted on the nose of a Terrier-Orion rocket launched from Woomera, South Australia.[1-2] Experimental data obtained from the flight test will be used to validate experimental data obtained in T4. This work is complimented with CFD studies performed at Seoul National University. The numerical results are compared to the correlation between aero-propulsion measurements made in the T4 hypersonic shock tunnel and the measurements made in free flight.

2. Intake Design Conditions

Flight conditions assume a Mach 7.6 flow which is deflected by an 18° wedge and is further compressed by a shock system. Experiments in the T4 shock tunnel use a nozzle with an exit Mach number of 6.5. To reproduce the combustion chamber entrance conditions expected during flight, a 17° compression wedge was used. The total enthalpy of the flow was almost the same as in flight. The intake schematic and station definition according to shock position are illustrated in Fig. 1.

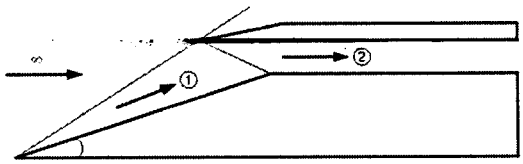

Fig. 1 Intake Schematic & Station Definitions

	h=35 km (T4/Flight)	h=28 km (T4/Flight)	h=23 km (T4/Flight)
P_∞ [kPa]	0.90/0.58	2.50/1.62	5.50/3.47
T_∞ [K]	310/237	298/225	288/220
a_∞ [m/s]	353.4/308.3	346.6/300.4	340.7/297.1
$h_{t\infty}$[MJ/kg]	2.95/2.98	2.84/2.83	2.74/2.77

Table 1 T4 Shock Tunnel and Flight Test Condition

Flight conditions from the US Standard Atmosphere and equivalent experimental conditions of T4 shock tunnel at each altitude are given in Table 1.

During the flight, the scramjet/rocket vehicle spins about its axis at 4 to 6 Hz and precesses slowly(0.1 Hz), resulting in an incoming flow deviation that may be as high as 8° (±4°angle of attack) in a worse-case scenario. The precessing of the vehicle could make instabilities develop. Such instabilities would be potentially disastrous to the experiment, and would need to be controlled. In the intake design, all flow cases that cover possible combination of three altitudes(35, 28, and 23km) and three angle of attacks (0° and ±4°) are considered. The design point corresponds to h=28km and 0° angle of attack.

h=28 km		P_F [kPa]	P_G [kPa]	E_P [%]	T_F [K]	T_G [K]	E_T [%]	M_F	M_G	E_M [%]
+4°	∞	1.62	2.50		224.5	298		7.6	6.5	
	②	100.01	100.32	0.31	1182.6	1188.5	0.50	2.63	2.63	0
0°	∞	1.62	2.50		224.5	298		7.6	6.5	
	②	85.85	84.14	1.98	1036.5	1050.7	1.35	2.95	2.93	0.68
-4°	∞	1.62	2.50		224.5	298		7.6	6.5	
	②	70.67	67.48	4.51	908.8	931.3	2.41	3.27	3.22	1.53

Table 2 Theoretical Calculations at On/Off-Design Cases using Oblique Shock Relation with Variable Properties (Design Condition: h=28km, M_∞=6.5, AOA=0° → M_2=3.0)

To validate the T4 experimental conditions with flight test conditions theoretical calculations at on/off-design cases were carried out using two methods. One is an oblique shock relation with constant properties and the other is the same one with variable properties. In hypersonic flow, the temperature behind shock systems can be very high but the shock relations with constant properties do not consider the high temperature effect on flow properties. Therefore, the shock relation with variable properties is more reasonable for the prediction of hypersonic flow and in this study all theoretical calculations used this method. Calculation results about on/off-design conditions are given in Table 2 and are confined to the cases with an altitude of 28km because of limited space. Subscript 'F' and 'G' mean 'flight test condition' and 'ground test condition' respectively. Table 2 shows a good agreement between flight results and ground results from the modified T4 experimental condition.

3. Numerical Methods

3.1 Governing Equations

The Reynolds-averaged Navier-Stokes equation with a two-equation turbulent model is considered. The governing equations are summarized in conservative vector forms as:

$$\frac{\partial Q}{\partial t}+\frac{\partial F}{\partial x}+\frac{\partial G}{\partial y}=\frac{\partial F_v}{\partial x}+\frac{\partial G_v}{\partial y}+W$$

In the present study, a turbulent viscosity is calculated by the Menter's SST (Shear Stress Transport) model.

3.2 Numerical Methods

The finite volume cell-vertex scheme is used for the spatial discretization. The viscous terms are expressed by a central difference method and the convective terms are expressed as a difference of the numerical fluxes at the cell interface. The numerical fluxes containing artificial dissipation are formulated using Roe's flux difference splitting (FDS) method. The MUSCL scheme is used for the extrapolation of primitive variables at the cell interface. In addition, the minmod limiter function is used to overcome the severe dispersion error introduced by the higher-order extrapolation and to preserve the total variation diminishing property. By applying the LU-SSOR method, governing equations can be integrated fully implicitly by the diagonal lower and upper steps with an approximate Jacobian splitting method.

4. Results

4.1 Intake Configuration Design

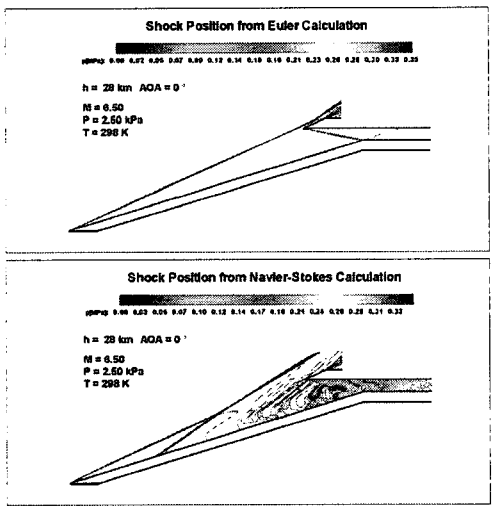

Fig. 2 Euler and Navier-Stokes Computation at Design Condition

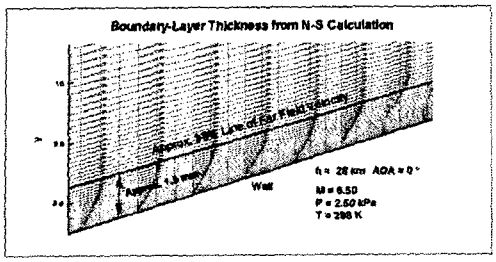

Fig 3 Boundary-Layer Thickness (h=28km, AOA=0°)

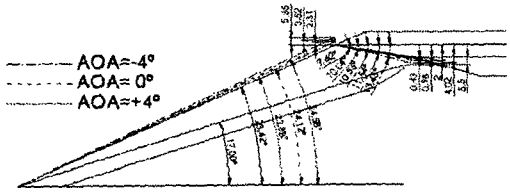

Fig. 4 Intake Configuration with Spillage Gap

Euler and Navier-Stokes computations based on T4 experimental conditions are carried out at the design point. The Euler computation shows a started mode. On the other hand, the Navier-Stokes computation including the boundary-layer solution shows an unstarted mode in Fig. 2. The strong cowl shock impinges the boundary-layer around a compression wedge corner and this causes the boundary-layer separation. This large separation zone induces an intake unstart and supersonic flow spillage. For proper intake operation the boundary-layer development and separation at the compression wedge need to be minimized. In the present study, a spillage gap is proposed to remove the boundary-layer separation and the impinging shock.

To properly design the spillage gap, the reflection of the impinging shock as a function of the angle of attack and the boundary-layer thickness is required. But excessive spillage gap can cause loss of airflow resulting in a lower intake efficiency. For the design of proper gap size, computations at different angles of attack are performed to measure the cowl shock impinging points. The boundary-layer thickness is calculated from Fig. 3. The spillage gap is determined through the measured impinging shock positions and the boundary-layer thickness, resulting in a final intake configuration as depicted in Fig. 4. A 4 mm offset is necessary for shock impingements, and a 1.5 mm margin is further added for boundary-layer thickness which reaches 95% of freestream velocity.

4.2 Simulation of Ground Tests

A matrix of 9 flow cases was identified that covers possible combination of three altitudes(35, 28, 23km) and three angles of attacks (0°, ±4°) with adiabatic wall boundary condition and fully turbulent boundary layer assumptions. A subset of 3 was chosen for performing a parametric CFD study of the influence of each of these three parameters.

Fig. 5 shows the static pressure contours and the stream traces in the vicinity of the cowl leading edge and bleed/combustor entrances, for the extreme cases of ±4° angle of attack at 28km altitude. The CFD computation and shadow graph show a good agreement with respect to shock position. Several features are visible in the figures: (i) the main intake shock passes outside the cowl (ii) the boundary-layer on the main intake surface is captured successfully by the spillage gap (iii) the cowl leading edge shock propagates into the spillage gap but is strongly diffracted by the corner expansion at the entrance to the gap (iv) a bow shock sits around the combustor leading edge, passing into the combustor on one side and into the spillage gap on the other side.

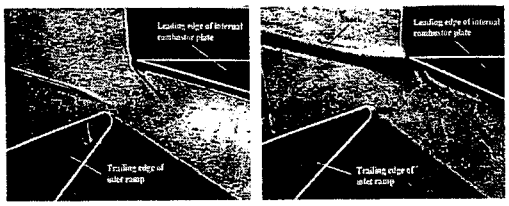

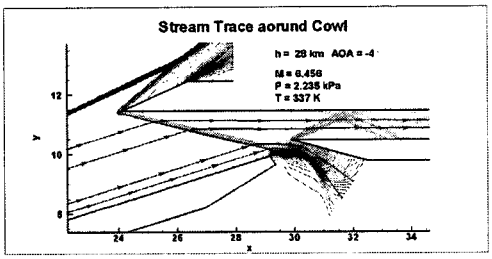

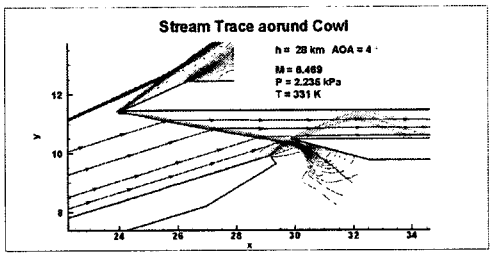

Fig. 5 Shock Position and Streamline Trace around Cowl (h=28km, AOA=±4°)

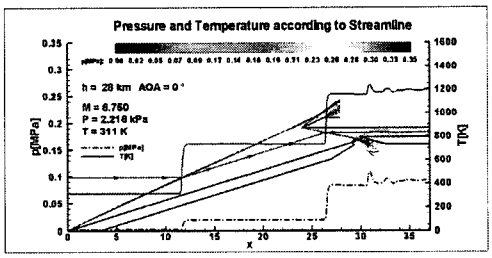

Fig. 6 Pressure and Temperature along the Streamline (h=28km, AOA=0°)

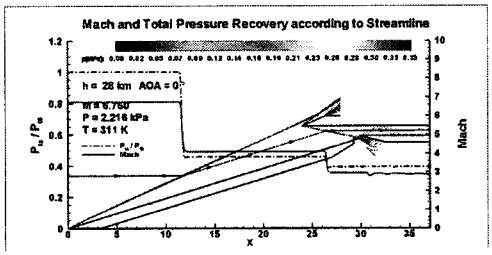

Fig. 7 Mach No. and Total Pressure Recovery along the Streamline (h=28km, AOA=0°)

Static pressure and temperature distribution for the case of 28km altitude and 0° angle of attack are presented in Fig. 6. Flow properties are extracted along the streamline originating from the combustor entrance mid-position. At the combustor entrance, uniform and stable pressure and temperature distribution are acquired in spite of combustor leading edge shock. The static pressure and static temperature midway between combustor walls are 91.2 kPa and 1187 K respectively. Fig. 7 indicates Mach No. and total pressure recovery for the same condition. Mach No. and total pressure recovery are also uniform and stable at a combustor entrance. The Mach No. is about 2.9 which approach the design point and total pressure recovery is approximately 39%.

Table 3 summarizes 4 different computations and the contents are confined to h=28 km cases because of space limitation. For convenience the explanation focus is on the design case. In the present study 4 intake calculation methods were used: (i) theoretical calculation with constant properties, (ii) theoretical calculation with variable properties, (iii) CFD results at just after the cowl shock and (iv) CFD results at combustor entrance. In the case of pressure, the values from each calculation are 82.07, 80.97, 83.47 and 91.19 kPa respectively. For the first calculation method, the value of 82.07 kPa is calculated by simple oblique shock relation without any modification. For the second calculation method, a pressure of 80.97 kPa is found considering a specific heat ratio varying with the temperature. As the flow temperature increases rapidly through the strong shocks, the specific heat ratio decreases. As a result of the decreased specific heat ratio, the pressure ratio also decreases before and after

Altitude	AOA	Theory (i)	Error[%]	Theory (ii)	Error[%]	CFD (iii)	Error[%]	CFD (iv)
28km	-4°	P= 89.53	9.1	P= 88.41	1.8	P= 90.59	0.1	P= 100.38
		M= 2.42		M= 2.65		M= 2.61		M= 2.55
		T= 1452.1		T= 1312.1		T= 1333.4		T= 1368.6
		$P_{t2}/P_{t\infty}$ 0.241		$P_{t2}/P_{t\infty}$ 0.350		$P_{t2}/P_{t\infty}$ 0.331		$P_{t2}/P_{t\infty}$ 0.332
	0°	P= 82.07	9.1	P= 80.97	4.1	P= 83.47	0.1	P= 91.19
		M= 2.79		M= 3.00		M= 2.95		M= 2.90
		T= 1228.9		T= 1135.9		T= 1159.5		T= 1186.9
		$P_{t2}/P_{t\infty}$ 0.302		$P_{t2}/P_{t\infty}$ 0.434		$P_{t2}/P_{t\infty}$ 0.392		$P_{t2}/P_{t\infty}$ 0.393
	+4°	P= 60.48	10.1	P= 59.59	6.7	P= 62.11	0.1	P= 69.06
		M= 3.05		M= 3.24		M= 3.17		M= 3.10
		T= 1084.1		T= 1017.6		T= 1044.4		T= 1074.5
		$P_{t2}/P_{t\infty}$ 0.426		$P_{t2}/P_{t\infty}$ 0.594		$P_{t2}/P_{t\infty}$ 0.526		$P_{t2}/P_{t\infty}$ 0.527

Table 3 Summary of Computations

a shock and this causes the pressure to be reduced to 80.97 kPa. For the third calculation method, the CFD pressure value just after the cowl shock reaches 83.47 kPa due to the boundary-layer development at the compression wedge increasing the oblique shock angle at the cowl (0.2° at each case). For the fourth calculation method, the pressure at the combustor entrance is of 91.19 kPa because the combustor channel area is contracted by the boundary-layer development. From the above results it can be concluded that the theoretical calculation with variable properties is useful for quick and simple prediction of flow properties but CFD computations are needed for detail flow characteristics like viscosity, boundary-layer effect and combustor entrance profile properties.

5. Conclusion

Computational fluid dynamics computations have been performed in support of the HyShot scramjet flight experiment. The CFD studies indicate that the intake bleed slot configuration performs well at all angle of attacks, with good agreements of shock position and boundary-layer/cowl-shock suction at the bleed between CFD and T4 shock tunnel experiment. As a result, stable and uniform pressure and temperature profiles are obtained at the combustor entrance. In addition, proper Mach number and total pressure recovery were maintained at the combustor entrance. The influence of the angle of attack on the flow properties is caused by the shock strength which controls most flow properties at the first compression wedge.

Acknowledgements

This work is a part of co-research with University of Queensland and Agency for Defense Development and supported by the BK21 of Seoul National University.

References

1. HyShot Scramjet Test Programme, http://www.mech.uq.edu.au/hyper/hyshot
2. Boyce, R. R., Paull, A., "Scramjet Intake and Exhaust CFD Studies for HyShot Scramjet Flight Experiment," AIAA-2001-189